Editors' Suggestion

Measurement of the Z-Boson Mass

R. Aaij *et al.*[*]
(LHCb Collaboration)

(Received 22 May 2025; revised 15 August 2025; accepted 15 September 2025; published 17 October 2025)

The first dedicated Z-boson mass measurement at the LHC with $Z \to \mu^+\mu^-$ decays is reported. The dataset uses proton-proton collisions at a center-of-mass energy of 13 TeV, recorded in 2016 by the LHCb experiment, and corresponds to an integrated luminosity of 1.7 fb^{-1}. A template fit to the $\mu^+\mu^-$ mass distribution yields the following result for the Z-boson mass: $m_Z = 91,185.7 \pm 8.3 \pm 3.9$ MeV, where the first uncertainty is statistical and the second systematic. This result is consistent with previous measurements and predictions from global electroweak fits.

DOI: 10.1103/ydn7-qx1d

In the standard model (SM) of particle physics the electroweak interactions are governed by $\mathrm{SU}(2) \times \mathrm{U}(1)$ local gauge symmetry, which is spontaneously broken when the Higgs field acquires a vacuum expectation value $v \approx 246$ GeV. The Z boson is a mixture of the SU(2) and U(1) gauge fields. At lowest order, its mass is given by $m_Z = \frac{1}{2} v (g^2 + g'^2)^{\frac{1}{2}}$, where g and g' are the SU(2) and U(1) gauge couplings, respectively. Including higher-order corrections and defining m_Z in a relativistic Breit–Wigner line shape with a mass-dependent width, a SM prediction of $m_Z = 91204.7 \pm 8.8$ MeV is obtained from a fit to precision electroweak data [1]. (Natural units, where $c = 1$, are used throughout this Letter.)

The most precise m_Z measurement, combining the data from the four LEP e^+e^- collider experiments, obtained $m_Z = 91187.6 \pm 2.1$ MeV [2]. The CDF collaboration reported a measurement of m_Z with a precision of 7 MeV, as a validation of their W-boson mass measurement [3]. A similar study by the CMS collaboration [4], while presented as not being fully independent of the previously known m_Z value, suggests encouraging prospects for a dedicated m_Z measurement.

This Letter reports the first dedicated measurement of m_Z at the LHC, using $Z \to \mu^+\mu^-$ decays recorded with the LHCb detector, in proton-proton collisions at a center-of-mass energy of 13 TeV. The LHCb detector [5,6] instruments the pseudorapidity range $2 < \eta < 5$ with a high-precision tracking system consisting of a silicon-strip vertex detector surrounding the proton-proton interaction region [7], a large-area silicon-strip detector (the TT) located upstream of a dipole magnet with a bending power of about 4 T m, and three stations of silicon-strip detectors and straw drift tubes [8] placed downstream of the magnet. The tracks are fitted with a Kalman filter that takes into account multiple scattering and corrects for energy loss due to ionization. For particles of charge q and momentum p, the typical q/p resolution is $\mathcal{O}(10^{-2})$ TeV^{-1}. This translates to a relative resolution of $\mathcal{O}(1\%)$ on the momenta, typically around 500 GeV, of muons from Z-boson decays in LHCb. Muons are identified by a dedicated system composed of alternating layers of iron and multiwire proportional chambers [9]. The energies of photons and hadrons are measured with a system of calorimeters.

The data were recorded in 2016 and correspond to an integrated luminosity of 1.7 fb^{-1}, divided between each of the two magnet-polarity configurations in roughly equal measure. The online event selection was performed by a trigger system [10,11], and this analysis uses events recorded by single-muon triggers. In order to prevent observer bias, the analysis was carried out by introducing an unknown offset in the m_Z value until the analysis methodology was finalized.

Simulation samples are generated using Pythia [12] with a specific LHCb configuration [13]. Decays of heavy particles, such as weak bosons and top quarks, are modeled directly with Pythia, while decays of lighter particles are described by EvtGen [14], in which final-state photon radiation is generated using Photos [15]. The interaction of the generated particles with the detector is implemented [16] using the Geant4 toolkit [17].

Candidate $Z \to \mu^+\mu^-$ decays are formed from pairs of oppositely charged muons, with invariant masses between 86 and 96 GeV. The muons must have transverse momenta $p_{\mathrm{T}} > 20$ GeV, $p < 2$ TeV, $2.2 < \eta < 4.4$, and their momenta must have relative uncertainties of less than 6%. Both muons must be consistent with originating from a primary collision vertex (PV) and have an "isolation" of less than 40 GeV. The isolation sums the transverse

[*]Full author list given at the end of the Letter.

momenta of all other particles for which the quadrature sum of the separation, with respect to the muon, in pseudorapidity and azimuthal angle is below 0.4. Around 174×10^3 candidates are selected by these requirements, which suppress the hadronic backgrounds to a negligible level with minimal signal inefficiency.

A sample of around 193×10^3 candidate $\Upsilon \to \mu^+\mu^-$ decays is used for the momentum calibration, while roughly 48×10^3 candidate $J/\psi \to \mu^+\mu^-$ decays are used for an independent cross-check. These quarkonium candidates are selected from pairs of oppositely charged muons with $p_{\mathrm{T}} > 5$ GeV and $2.2 < \eta < 4.4$. The p_{T} requirements, which are tighter than those typically used in analyses of Υ and J/ψ decays in LHCb, select a subset of muons that are more similar to those from Z -boson decays. Muon-isolation requirements are not imposed since quarkonium states tend to be produced in hadronic jets [18], but all other muon-quality requirements from the Z-boson selection are applied. The J/ψ candidates are required to have a significant displacement from the PV and, therefore, originate predominantly from decays of beauty hadrons.

To highlight the importance of the momentum calibration in this analysis, briefly assume the limit of massless muons in which the dimuon mass m is given by $m^2 \simeq 2p^+p^-(1-\cos\theta)$ with $p^\pm$ denoting the $\mu^\pm$ momenta and θ being the angle between the muons, which is measured with very high precision. The main challenge is to control systematic biases on the $p^\pm$ measurements. To a good approximation, these transform the measured momenta of particles with charge q as

$$p \to (1 + \alpha + \beta/p - q\delta p)p, \tag{1}$$

where α is a momentum-scale offset caused by a miscalibration of the bending power of the magnet and/or the tracker length scale; β is due to a possible inaccuracy in the ionisation-energy-loss corrections; and δ is a q/p bias due to a misalignment of the tracking detectors. These parameters may vary between different detector regions.

A general-purpose momentum calibration for LHCb [19] achieves a relative uncertainty of 3×10^{-4} for application to a wide range of decays with different lifetimes and final-state particle momenta. The present analysis requires a dedicated calibration with a higher precision specifically for high-p_{T} muons and with an emphasis on differences between data and simulation. This calibration is performed in four stages, the first of which uses the $Z \to \mu^+\mu^-$ sample, without an assumption on the m_Z value, while the remaining three use the $\Upsilon \to \mu^+\mu^-$ sample. The first two calibrations apply to the data, and the last two subsequently apply to the simulation.

The first momentum calibration estimates the charge-dependent curvature biases (δ) with $Z \to \mu^+\mu^-$ decays and the pseudomass method [20,21]. Denoting the $\mu^\pm$ momentum and transverse momentum as $p^\pm$ and $p_{\mathrm{T}}{}^\pm$, respectively, the two pseudomasses, defined as

$$\mathcal{M}^\pm \equiv \sqrt{2p^\pm p_{\mathrm{T}}^\pm \frac{p^\mp}{p_{\mathrm{T}}^\mp}(1-\cos\theta)}, \tag{2}$$

estimate the dimuon mass under the assumption of a relatively small dimuon transverse momentum. In intervals of η, ϕ, and the magnet polarity, a simultaneous fit of the $\mathcal{M}^+$ and $\mathcal{M}^-$ distributions determines the charge asymmetry in the peak positions, which is multiplied by a factor of $-\frac{1}{2}(\langle 1/p^+\rangle + \langle 1/p^-\rangle)$ to estimate δ, where $\langle 1/p^\pm\rangle$ are the mean values of the inverse of the muon momenta. A small bias in the δ estimates [20], which is an order of magnitude smaller than the dominant misalignment effect, is corrected with simulation as in Ref. [22]. Applying the corrected δ values to the muon momenta in data improves the Z mass resolution by $\mathcal{O}(20\%)$. Crucially, it is verified that variations as large as ± 100 MeV in the m_Z value of 91,187.6 MeV assumed in the simulation have an effect of less than 1 MeV on the m_Z measurement.

The second momentum calibration accounts for a relative momentum-scale drift of $\mathcal{O}(10^{-4})$ during the data taking. The Υ-meson sample is divided into 20 data-taking periods, and the mass distributions are modeled with a fit function composed of two Crystal Ball functions [23] for the signal and an exponential for the background. The two signal functions share a common peak-position parameter, but differ by a relative-width factor, which varies freely in the fit together with their relative normalization. The peak position is parametrized as the known Υ mass [24], multiplied by $(1+\alpha)$. The momenta in data are corrected according to the 20 values for α from these fits, which are shown in Fig. 3 in the Appendix.

The third momentum calibration accounts for a possible underestimation in the simulation of the α variations across the detector. Corrections are defined according to 16 discrete "directions," which correspond to the product of four intervals in the range $2.2 < \eta < 4.4$ and four ϕ intervals. The Υ-meson sample is divided into 116 subsamples according to the μ^+ and μ^- directions, after folding across the diagonal and, subsequently, removing 20 subsamples with fewer than 100 candidates in data. Mass measurements are obtained for these 116 subsamples using the same fit model as in the drift calibration. The 16 values of α are determined from a χ^2 fit in which the measured mass for the subsample with the $\mu^+(\mu^-)$ being in the directional interval $i(j)$ is predicted to differ from the known Υ mass [24] by a factor $\sqrt{(1+\alpha_i)(1+\alpha_j)}$.

Figure 4 in the Appendix shows that, in the fit to data, localized α values as large as $\pm 10^{-3}$ are estimated, and the χ^2 of the fit is roughly 700 units smaller than that where a single α value is used. The variations in the simulation are

an order of magnitude smaller, and these are subsequently corrected to match those seen in data.

The final, and most important stage, of the momentum calibration simultaneously determines an overall α correction and the coefficients $\sigma_{1,2}$ of two momentum smearing factors for the simulation. The first smearing factor, which accounts for a small underestimation of the multiple scattering in simulation, has the form $[1 + f(\eta)\mathcal{R}_1\sigma_1]$, where $\mathcal{R}_1$ is a random number sampled from a standard normal distribution, and $f(\eta)$ is defined as 1.0 (1.5) for muons with η below (above) 3.3, roughly following an increase in the number of radiation lengths traversed by charged particles. The second smearing factor, which accounts for an overly idealized q/p resolution in the simulation, has the form $(1 + \mathcal{R}_2 p\sigma_2/\cosh\eta)$, where $\mathcal{R}_2$ is another normally distributed random number. A fit minimizes the χ^2 between the Υ mass distribution in data and simulation, depending on the values of α and $\sigma_{1,2}$ used to smear the momenta in the simulation. In this fit, the Υ mass in the simulation is shifted by $+0.1$ MeV from the default value of 9460.3 MeV to the current known value [24]. The background is modeled with an exponential function with a freely varying slope and normalization. The χ^2 of the fit is 76 for 95 degrees of freedom. Figure 1 shows the Υ mass distribution in data, compared to the simulation before and after smearing with the best-fit values of $\alpha = (-0.65 \pm 0.16) \times 10^{-4}$, $\sigma_1 = (1.98 \pm 0.07) \times 10^{-3}$, and $\sigma_2 = 0.147 \pm 0.009$ TeV^{-1}. Despite the preceding calibrations, the negative α value can be understood as follows: a shift of roughly -10^{-5} is attributed to the change in the Υ mass, while the remaining shift is attributed to a subtle anticorrelation of around -12% between α and σ_2, which is fixed to zero in the earlier stages.

Weights are assigned to the simulated candidates to correct for small inaccuracies in the modeling of the detection efficiency. Following the approaches of Refs. [22,25], these weights are derived from estimates of the track reconstruction, muon identification, and trigger efficiencies. These corrections are determined from samples of $Z \to \mu^+\mu^-$ and $\Upsilon \to \mu^+\mu^-$ decays in η and ϕ intervals, with parametrizations of the p_T dependence. The tracking and identification efficiency corrections are typically within 1% of unity, but the trigger efficiencies are overestimated by up to $\mathcal{O}(10\%)$ at the largest η values considered in this analysis.

The m_Z measurement is obtained from a χ^2 fit to the dimuon mass distribution in 40 intervals between 86 and 96 GeV, shown in Fig. 2. Backgrounds from $Z \to \tau^+\tau^-$, top-quark decays, vector-boson pairs, and hadrons are included, with their total fraction being $\mathcal{O}(10^{-3})$. The signal and background components are modeled with templates from the simulation samples with the calibrations already described. The signal normalization is allowed to vary freely in the fit.

Auxiliary signal samples without detector simulation are produced using a version of Powheg-Box [26–28] that includes next-to-leading-order corrections in the strong and electroweak couplings [29,30]. The NNPDF3.1 [31] parton distribution functions are used, and the samples are processed with Photos [32] for modeling of additional photon radiation and with Pythia [12] for simulating the rest of the event. Normalized mass distributions are produced for m_Z values of 91.1, 91.2, and 91.3 GeV in the G_μ input scheme [33]. These are divided by the distribution corresponding to the main simulation sample to make three ratio histograms, each of which is translated to event weights for the main simulation sample, evaluated

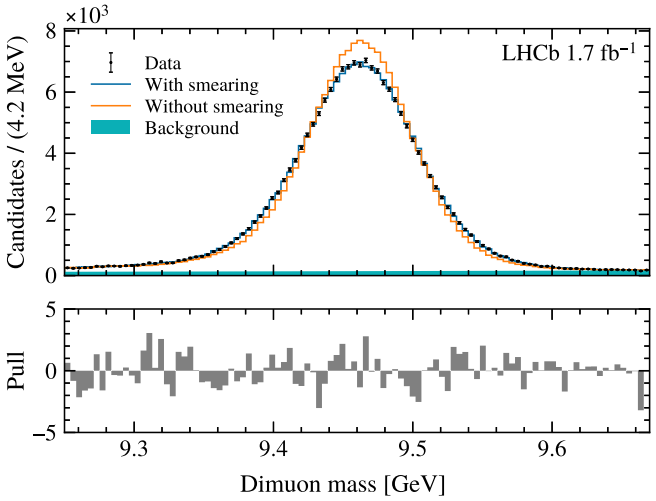

FIG. 1. Mass distribution of the $\Upsilon \to \mu^+\mu^-$ candidates, compared to the result of the momentum smearing fit, which includes a background component. The sum of the background and Υ signal simulation is also shown before momentum smearing.

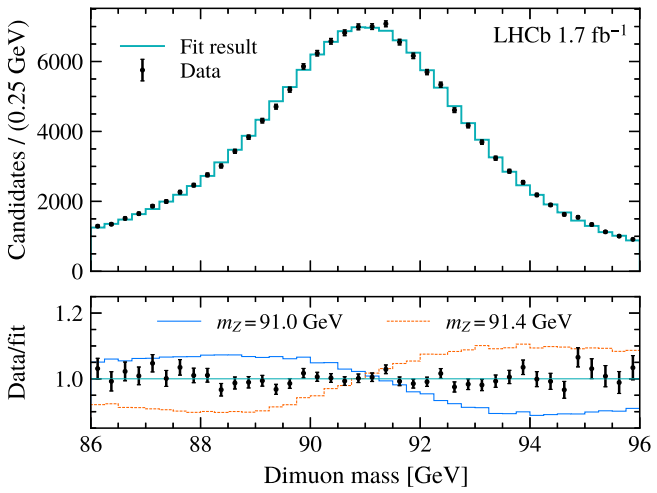

FIG. 2. Mass distribution of the $Z \to \mu^+\mu^-$ candidates, compared to predictions for two different m_Z values and to the results of the fit. The predictions and fit results include the small background component.

TABLE I. Systematic uncertainties on the m_Z measurement.

Source	Uncertainty [MeV]
Momentum calibration	3.6
Theory template statistics	1.0
Signal final-state radiation	1.0
Parton distribution functions	0.7
Detection efficiency	0.1
Total systematic uncertainty	3.9

as a function of the true mass. The momentum smearing fit precisely determines α, but the two σ parameters are less precisely determined from the Υ-meson samples. Therefore, σ_2, which is far more influential than σ_1 for the higher-momentum muons from Z-boson decays, varies freely by a factor f in the fit. Cubic-spline interpolation is used to continuously vary m_Z and f in the fit. The fit has a minimum χ^2/ndf of $43.4/37$, and the best fit values are $m_Z = 91,185.7 \pm 8.3$ MeV and $f = 1.2 \pm 0.1$, with a correlation coefficient of 0.015, where the uncertainties are statistical only. Figure 2 shows the result of this fit compared to the distribution in data.

Table I summarizes the systematic uncertainties on m_Z, in which the total is the combination in quadrature of the individual components. Most sources of systematic uncertainty are predominantly statistical and will decrease in future analyses of larger datasets. The largest source of uncertainty is attributed to the momentum calibration, described in more detail in the next paragraph. The next source of systematic uncertainty is attributed to the statistical precision of the true dimuon mass distributions used to define the weights for the simulated events. An uncertainty for the electroweak corrections in the signal model is estimated by repeating the fit with a model in which the photon radiation, beyond the electroweak corrections modeled directly by Powheg, is handled by Pythia instead of Photos. The shift in the m_Z value, which has a statistical uncertainty of 0.7 MeV, is assigned as the systematic uncertainty. The uncertainty due to the parton distribution functions is assessed from the envelope of fit results also including those based on the CT18 [34] and MSHT20 [35] sets. The detection efficiency uncertainty is obtained by propagating the statistical uncertainties in the estimated efficiencies.

The dominant momentum calibration uncertainty comprised five lower-level sources that are combined in quadrature. An uncertainty of 2.6 MeV is evaluated for the detector material description in the simulation. Variations of $\pm 10\%$ in the number of radiation lengths upstream of the magnet are emulated with values of β, set to zero by default, of ± 2 MeV applied to the simulation. While the β parameter has vanishing influence on the muons from Z-boson decays, it influences the determination of the α parameter in the momentum smearing fit. An uncertainty of 1.8 MeV results from propagating the covariance of the three parameters from the momentum smearing fit. The propagation of the uncertainty on the known Υ-meson mass [24] results in an uncertainty of 1.5 MeV. An uncertainty of 0.7 MeV is estimated by propagating the statistical uncertainties on the δ bias corrections. Finally, the difference between the Pythia and Photos descriptions of final-state photon radiation in the Υ simulation results in an uncertainty of 0.6 MeV.

Several cross-checks are performed to validate the measurement and its uncertainty. The m_Z fit is repeated with the samples divided into roughly equal-size pairs of subsamples according to the magnet polarity, the number of clusters in the scintillator-preshower detector, the number of tracks in the PV, and the angle between the decay plane and the y component of the magnetic field. The sample is also divided according to the opening angle between the muons, the sign of the difference between the muon pseudorapidities, the dimuon p_T, and the dimuon rapidity. Finally, the sample is split according to eight variables for each muon: the number of TT clusters, track-fit χ^2/ndf, momentum, and p_T, the relative uncertainty on the measured momentum, isolation, the consistency of the muons with a PV, and pseudorapidity. Figure 5 shows that the m_Z values corresponding to the subsamples differ by less than two standard deviations in all cases, where only the statistical uncertainties are accounted for. The m_Z fit is also repeated in four intervals of the angle ϕ of the μ^-, and these are consistent within two standard deviations.

For the momentum-scale calibrations and the momentum smearing fit, it is verified that repeating the fit, having applied the calibration, results in momentum-scale parameters consistent with zero. Several variations in the numbers of η and ϕ intervals in the third momentum calibration are tested. The largest variation in m_Z is 2 MeV, but this corresponds to an extreme reduction in the number of intervals, which causes an obvious deficiency in the simulation to be uncorrected. Therefore, no systematic uncertainty is assigned to this third calibration. The m_Z fit is tested with simulated events as pseudodata, validating the coverage of the uncertainty and ruling out any bias. This test is repeated with a wide range of m_Z values in the pseudodata, ruling out any significant nonlinear dependence. Reasonable variations in the number of mass intervals in the m_Z fit have a negligible effect on the results. The m_Z fit is tested with smaller (88 to 94 GeV) and larger (84 to 98 GeV) fit ranges than that of the baseline fit, and all results are consistent within two standard deviations. Finally, the m_Z measurement is repeated with two independent samples used in the momentum calibration and its uncertainty assessment. The first is $J/\psi \to \mu^+\mu^-$ decays with the same muon requirements as the default Υ sample. The second is $\Upsilon \to \mu^+\mu^-$ decays where both muons satisfy $p_T > 3$ GeV but one fails the default requirement of $p_T > 5$ GeV. Figure 6 shows that the systematic uncertainties are larger with these alternative samples and the central m_Z values are consistent with the baseline result within 2 MeV.

In summary, the first dedicated measurement of the Z-boson mass at the LHC is presented. This is based on a template fit to the mass distribution of $Z \to \mu^+\mu^-$ decays, in a dataset recorded by the LHCb experiment in 2016, corresponding to an integrated luminosity of 1.7 fb^{-1}. The momentum calibration is primarily based on a sample of $\Upsilon \to \mu^+\mu^-$ decays. The resulting measurement of the Z-boson mass is

$$m_Z = 91,185.7 \pm 8.3 \pm 3.9 \text{ MeV},$$

where the first uncertainty is statistical and the second systematic. This result is consistent with previous measurements, and it is consistent with, and matches the precision of, the predictions of the global electroweak fits. The unique design of the LHCb detector means that the uncertainties are expected to be mostly uncorrelated with potential measurements of the Z-boson mass by the other LHC experiments. Since its uncertainty is predominantly statistical, this result demonstrates encouraging prospects for analyses with larger LHCb datasets, with roughly an order of magnitude more data having already been recorded, and roughly two orders of magnitude projected after the high-luminosity LHC phase. Further work will be required to reduce the detector material uncertainty, but it is now conceivable that LHCb could challenge the precision of the LEP Z-boson mass determination in the future.

Acknowledgments—We express our gratitude to our colleagues in the CERN accelerator departments for the excellent performance of the LHC. We thank the technical and administrative staff at the LHCb institutes. We acknowledge support from CERN and from the national agencies: ARC (Australia); CAPES, CNPq, FAPERJ, and FINEP (Brazil); MOST and NSFC (China); CNRS/IN2P3 (France); BMBF, DFG, and MPG (Germany); INFN (Italy); NWO (Netherlands); MNiSW and NCN (Poland); MCID/IFA (Romania); MICIU and AEI (Spain); SNSF and SER (Switzerland); NASU (Ukraine); STFC (United Kingdom); DOE NP and NSF (USA). We acknowledge the computing resources that are provided by ARDC (Australia), CBPF (Brazil), CERN, IHEP, and LZU (China), IN2P3 (France), KIT and DESY (Germany), INFN (Italy), SURF (Netherlands), Polish WLCG (Poland), IFIN-HH (Romania), PIC (Spain), CSCS (Switzerland), and GridPP (United Kingdom). We are indebted to the communities behind the multiple open-source software packages on which we depend. Individual groups or members have received support from Key Research Program of Frontier Sciences of CAS, CAS PIFI, CAS CCEPP, Fundamental Research Funds for the Central Universities, and Sci. & Tech. Program of Guangzhou (China); Minciencias (Colombia); EPLANET, Marie Skłodowska-Curie Actions, ERC, and NextGenerationEU (European Union); A*MIDEX, ANR, IPhU and Labex P2IO, and Région Auvergne-Rhône-Alpes (France); Alexander-von-Humboldt Foundation (Germany); ICSC (Italy); Severo Ochoa and María de Maeztu Units of Excellence, GVA, XuntaGal, GENCAT, InTalent-Inditex, and Prog. Atracción Talento CM (Spain); SRC (Sweden); the Leverhulme Trust, the Royal Society, and UKRI (United Kingdom).

Data availability—The data that support the findings of this article are openly available [36], embargo periods may apply.

[1] J. de Blas, M. Ciuchini, E. Franco, A. Goncalves, S. Mishima, M. Pierini, L. Reina, and L. Silvestrini, Global analysis of electroweak data in the standard model, Phys. Rev. D **106**, 033003 (2022).
[2] S. Schael *et al.* (ALEPH, DELPHI, L3, OPAL, SLD Collaborations, LEP Electroweak Working Group, SLD Electroweak Group, and SLD Heavy Flavour Group), Precision electroweak measurements on the Z resonance, Phys. Rep. **427**, 257 (2006).
[3] T. Aaltonen *et al.* (CDF Collaboration), High-precision measurement of the W boson mass with the CDF II detector, Science **376**, 170 (2022).
[4] V. Chekhovsky *et al.* (CMS Collaboration), High-precision measurement of the W boson mass with the CMS experiment at the LHC, arXiv:2412.13872.
[5] A. A. Alves Jr. *et al.* (LHCb Collaboration), The LHCb detector at the LHC, J. Instrum. **3**, S08005 (2008).
[6] LHCb Collaboration, LHCb detector performance, Int. J. Mod. Phys. A **30**, 1530022 (2015).
[7] R. Aaij *et al.*, Performance of the LHCb vertex locator, J. Instrum. **9**, P09007 (2014).
[8] P. d'Argent *et al.*, Improved performance of the LHCb outer tracker in LHC run 2, J. Instrum. **12**, P11016 (2017).
[9] A. A. Alves, Jr. *et al.*, Performance of the LHCb muon system, J. Instrum. **8**, P02022 (2013).
[10] R. Aaij *et al.*, The LHCb trigger and its performance in 2011, J. Instrum. **8**, P04022 (2013).
[11] R. Aaij *et al.*, Design and performance of the LHCb trigger and full real-time reconstruction in Run 2 of the LHC, J. Instrum. **14**, P04013 (2019).
[12] T. Sjöstrand, S. Mrenna, and P. Skands, A brief introduction to Pythia 8.1, Comput. Phys. Commun. **178**, 852 (2008); Pythia 6.4 physics and manual, J. High Energy Phys. 05 (2006) 026.
[13] I. Belyaev *et al.*, Handling of the generation of primary events in Gauss, the LHCb simulation framework, J. Phys. Conf. Ser. **331**, 032047 (2011).
[14] D. J. Lange, The EvtGen particle decay simulation package, Nucl. Instrum. Methods Phys. Res., Sect. A **462**, 152 (2001).
[15] N. Davidson, T. Przedzinski, and Z. Was, Photos interface in C++: Technical and physics documentation, Comput. Phys. Commun. **199**, 86 (2016).
[16] M. Clemencic, G. Corti, S. Easo, C. R. Jones, S. Miglioranzi, M. Pappagallo, and P. Robbe, The LHCb simulation application, Gauss: Design, evolution and experience, J. Phys. Conf. Ser. **331**, 032023 (2011).

[17] J. Allison *et al.* (Geant4 Collaboration), Geant4 developments and applications, IEEE Trans. Nucl. Sci. **53**, 270 (2006); S. Agostinelli *et al.* (Geant4 Collaboration), Geant4: A simulation toolkit, Nucl. Instrum. Methods Phys. Res., Sect. A **506**, 250 (2003).
[18] R. Aaij *et al.* (LHCb Collaboration), Study of J/ψ production in jets, Phys. Rev. Lett. **118**, 192001 (2017).
[19] R. Aaij *et al.* (LHCb Collaboration), Momentum scale calibration of the LHCb spectrometer, J. Instrum. **19**, P02008 (2024).
[20] W. Barter, M. Pili, and M. Vesterinen, A simple method to determine curvature biases in track reconstruction in hadron collider experiments, Eur. Phys. J. C **81**, 251 (2021).
[21] R. Aaij *et al.* (LHCb Collaboration), Charge-dependent curvature-bias corrections using a pseudomass method, J. Instrum. **19**, P03010 (2024).
[22] R. Aaij *et al.* (LHCb Collaboration), Measurement of the effective leptonic weak mixing angle, J. High Energy Phys. 12 (2024) 026.
[23] T. Skwarnicki, A study of the radiative cascade transitions between the Upsilon-prime and Upsilon resonances, Ph.D. thesis, Institute of Nuclear Physics, Krakow, 1986, DESY-F31-86-02.
[24] S. Navas *et al.* (Particle Data Group), Review of particle physics, Phys. Rev. D **110**, 030001 (2024).
[25] R. Aaij *et al.* (LHCb Collaboration), Measurement of the W boson mass, J. High Energy Phys. 01 (2022) 036.
[26] P. Nason, A new method for combining NLO QCD with shower Monte Carlo algorithms, J. High Energy Phys. 11 (2004) 040.
[27] S. Frixione, P. Nason, and C. Oleari, Matching NLO QCD computations with parton shower simulations: The Powheg method, J. High Energy Phys. 11 (2007) 070.
[28] S. Alioli, P. Nason, C. Oleari, and E. Re, A general framework for implementing NLO calculations in shower Monte Carlo programs: the Powheg Box, J. High Energy Phys. 06 (2010) 043.
[29] L. Barze, G. Montagna, P. Nason, O. Nicrosini, F. Piccinini, and A. Vicini, Neutral current Drell–Yan with combined QCD and electroweak corrections in the Powheg Box, Eur. Phys. J. C **73**, 2474 (2013).
[30] M. Chiesa, C. L. Del Pio, and F. Piccinini, On electroweak corrections to neutral current Drell–Yan with the Powheg Box, Eur. Phys. J. C **84**, 539 (2024).
[31] R. D. Ball *et al.* (NNPDF Collaboration), Parton distributions from high-precision collider data, Eur. Phys. J. C **77**, 663 (2017).
[32] E. Barberio, B. van Eijk, and Z. Was, Photos: A universal Monte Carlo for QED radiative corrections in decays, Comput. Phys. Commun. **66**, 115 (1991).
[33] M. Chiesa, F. Piccinini, and A. Vicini, Direct determination of $\sin^2\theta^{\ell}_{\rm eff}$ at hadron colliders, Phys. Rev. D **100**, 071302(R) (2019).
[34] T.-J. Hou *et al.*, New CTEQ global analysis of quantum chromodynamics with high-precision data from the LHC, Phys. Rev. D **103**, 014013 (2021).
[35] S. Bailey, T. Cridge, L. A. Harland-Lang, A. D. Martin, and R. S. Thorne, Parton distributions from LHC, HERA, Tevatron and fixed target data: MSHT20 PDFs, Eur. Phys. J. C **81**, 341 (2021).
[36] https://cds.cern.ch/record/2932727

End Matter

Appendix—Figure 3 shows the momentum-scale correction factors in data-taking period intervals. Figure 4 shows the directional momentum-scale offsets for data and simulation. Figure 5 shows the pulls for a set of cross-checks where the samples are divided into two subsamples of roughly equal size. Figure 6 shows the m_Z results based on three different calibration samples.

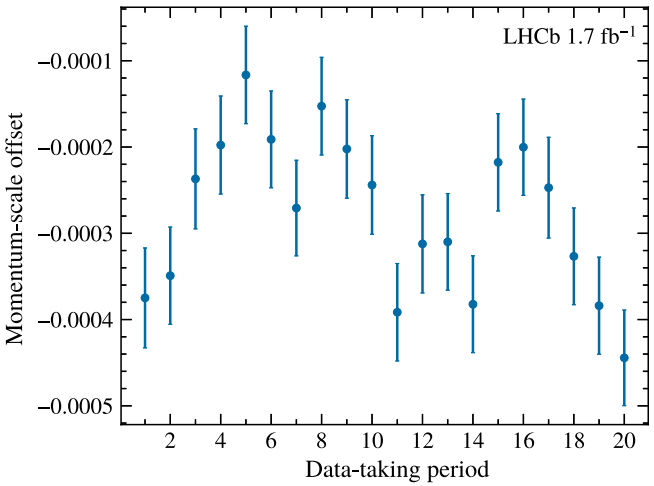

FIG. 3. Momentum-scale offset, corresponding to α in Eq. (1), in data-taking periods for data.

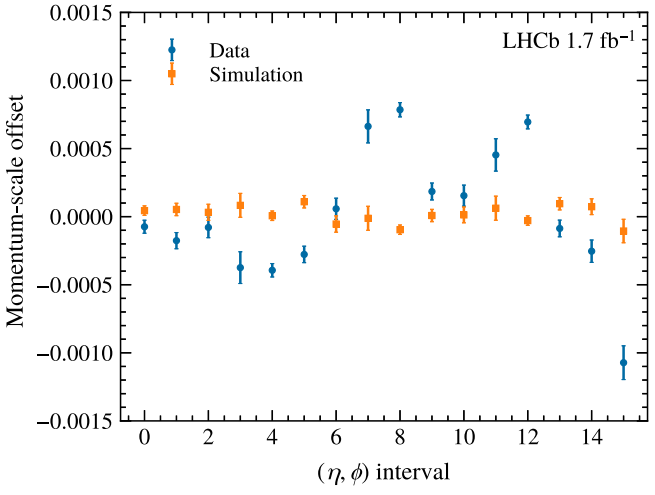

FIG. 4. Momentum-scale offsets, corresponding to α in Eq. (1), for data and simulation, in intervals of muon pseudorapidity (η) and azimuthal angle (ϕ).

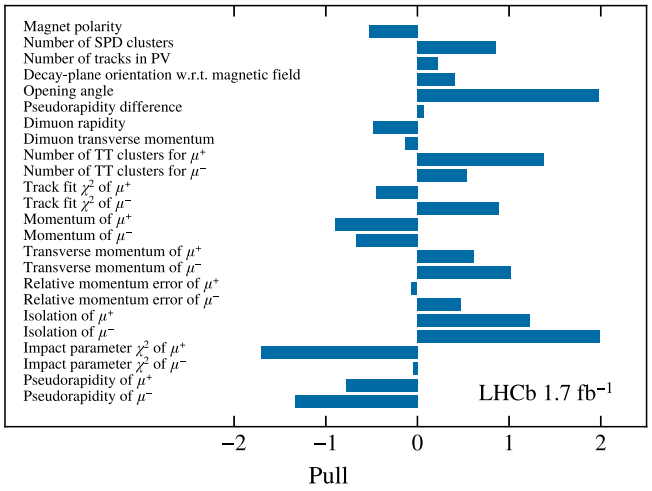

FIG. 5. Summary of cross-checks where the data are divided into subsamples of approximately equal size. The pull is defined as the difference between the measurements of a pair of subsamples divided by the sum in quadrature of their statistical uncertainties.

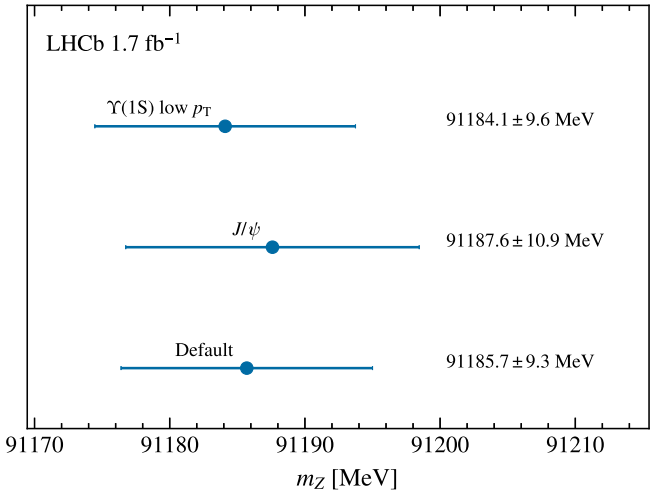

FIG. 6. Measurements of m_Z with the baseline calibration sample and two alternatives. The uncertainties correspond to the quadrature sum of statistical and systematic sources. For the J/ψ sample, the uncertainty on the known Υ mass is replaced with that for the J/ψ meson. The final-state-radiation uncertainty is also adapted for the specific J/ψ-meson decay model.

R. Aaij,[38] A. S. W. Abdelmotteleb,[57] C. Abellan Beteta,[51] F. Abudinén,[57] T. Ackernley,[61] A. A. Adefisoye,[69] B. Adeva,[47] M. Adinolfi,[55] P. Adlarson,[84] C. Agapopoulou,[14] C. A. Aidala,[86] Z. Ajaltouni,[11] S. Akar,[11] K. Akiba,[38] P. Albicocco,[28] J. Albrecht,[19,b] F. Alessio,[49] Z. Aliouche,[63] P. Alvarez Cartelle,[56] R. Amalric,[16] S. Amato,[3] J. L. Amey,[55] Y. Amhis,[14] L. An,[6] L. Anderlini,[27] M. Andersson,[51] P. Andreola,[51] M. Andreotti,[26] A. Anelli,[31,49,c] D. Ao,[7] F. Archilli,[37,d] Z Areg,[69] M. Argenton,[26] S. Arguedas Cuendis,[9,49] A. Artamonov,[44] M. Artuso,[69] E. Aslanides,[13] R. Ataíde Da Silva,[50] M. Atzeni,[65] B. Audurier,[12] D. Bacher,[64] I. Bachiller Perea,[50] S. Bachmann,[22] M. Bachmayer,[50] J. J. Back,[57] P. Baladron Rodriguez,[47] V. Balagura,[15] A. Balboni,[26] W. Baldini,[26] L. Balzani,[19] H. Bao,[7] J. Baptista de Souza Leite,[61] C. Barbero Pretel,[47,12] M. Barbetti,[27] I. R. Barbosa,[70] R. J. Barlow,[63] M. Barnyakov,[25] S. Barsuk,[14] W. Barter,[59] J. Bartz,[69] S. Bashir,[40] B. Batsukh,[5] P. B. Battista,[14] A. Bay,[50] A. Beck,[65] M. Becker,[19] F. Bedeschi,[35] I. B. Bediaga,[2] N. A. Behling,[19] S. Belin,[47] K. Belous,[44] I. Belov,[29] I. Belyaev,[36] G. Benane,[13] G. Bencivenni,[28] E. Ben-Haim,[16] A. Berezhnoy,[44] R. Bernet,[51] S. Bernet Andres,[46] A. Bertolin,[33] C. Betancourt,[51] F. Betti,[59] J. Bex,[56] Ia. Bezshyiko,[51] O. Bezshyyko,[85] J. Bhom,[41] M. S. Bieker,[18] N. V. Biesuz,[26] P. Billoir,[16] A. Biolchini,[38] M. Birch,[62] F. C. R. Bishop,[10] A. Bitadze,[63] A. Bizzeti,[27,e] T. Blake,[57,f] F. Blanc,[50] J. E. Blank,[19] S. Blusk,[69] V. Bocharnikov,[44] J. A. Boelhauve,[19] O. Boente Garcia,[15] T. Boettcher,[68] A. Bohare,[59] A. Boldyrev,[44] C. S. Bolognani,[81] R. Bolzonella,[26] R. B. Bonacci,[1] N. Bondar,[44,49] A. Bordelius,[49] F. Borgato,[33,49] S. Borghi,[63] M. Borsato,[31,c] J. T. Borsuk,[82] E. Bottalico,[61] S. A. Bouchiba,[50] M. Bovill,[64] T. J. V. Bowcock,[61] A. Boyer,[49] C. Bozzi,[26] J. D. Brandenburg,[87] A. Brea Rodriguez,[50] N. Breer,[19] J. Brodzicka,[41] A. Brossa Gonzalo,[47,a] J. Brown,[61] D. Brundu,[32] E. Buchanan,[59] L. Buonincontri,[33,g] M. Burgos Marcos,[81] A. T. Burke,[63] C. Burr,[49] J. S. Butter,[56] J. Buytaert,[49] W. Byczynski,[49] S. Cadeddu,[32] H. Cai,[74] A. Caillet,[16] R. Calabrese,[26,h] S. Calderon Ramirez,[9] L. Calefice,[45] S. Cali,[28] M. Calvi,[31,c] M. Calvo Gomez,[46] P. Camargo Magalhaes,[2,i] J. I. Cambon Bouzas,[47] P. Campana,[28] D. H. Campora Perez,[81] A. F. Campoverde Quezada,[7] S. Capelli,[31] L. Capriotti,[26] R. Caravaca-Mora,[9] A. Carbone,[25,j] L. Carcedo Salgado,[47] R. Cardinale,[29,k] A. Cardini,[32] P. Carniti,[31] L. Carus,[22] A. Casais Vidal,[65] R. Caspary,[22] G. Casse,[61] M. Cattaneo,[49] G. Cavallero,[26,49] V. Cavallini,[26,h] S. Celani,[22] S. Cesare,[30,l] A. J. Chadwick,[61] I. Chahrour,[86] H. Chang,[4,m] M. Charles,[16]

Ph. Charpentier,[49] E. Chatzianagnostou,[38] M. Chefdeville,[10] C. Chen,[56] S. Chen,[5] Z. Chen,[7] A. Chernov,[41] S. Chernyshenko,[53] X. Chiotopoulos,[81] V. Chobanova,[83] M. Chrzaszcz,[41] A. Chubykin,[44] V. Chulikov,[28,36] P. Ciambrone,[28] X. Cid Vidal,[47] G. Ciezarek,[49] P. Cifra,[38] P. E. L. Clarke,[59] M. Clemencic,[49] H. V. Cliff,[56] J. Closier,[49] C. Cocha Toapaxi,[22] V. Coco,[49] J. Cogan,[13] E. Cogneras,[11] L. Cojocariu,[43] S. Collaviti,[50] P. Collins,[49] T. Colombo,[49] M. Colonna,[19] A. Comerma-Montells,[45] L. Congedo,[24] A. Contu,[32] N. Cooke,[60] C. Coronel,[66] I. Corredoira,[12] A. Correia,[16] G. Corti,[49] J. Cottee Meldrum,[55] B. Couturier,[49] D. C. Craik,[51] M. Cruz Torres,[2,n] E. Curras Rivera,[50] R. Currie,[59] C. L. Da Silva,[68] S. Dadabaev,[44] L. Dai,[71] X. Dai,[4] E. Dall'Occo,[49] J. Dalseno,[83] C. D'Ambrosio,[62] J. Daniel,[11] P. d'Argent,[24] G. Darze,[3] A. Davidson,[57] J. E. Davies,[63] O. De Aguiar Francisco,[63] C. De Angelis,[32,o] F. De Benedetti,[49] J. de Boer,[38] K. De Bruyn,[80] S. De Capua,[63] M. De Cian,[63] U. De Freitas Carneiro Da Graca,[2,p] E. De Lucia,[28] J. M. De Miranda,[2] L. De Paula,[3] M. De Serio,[24,q] P. De Simone,[28] F. De Vellis,[19] J. A. de Vries,[81] F. Debernardis,[24] D. Decamp,[10] S. Dekkers,[1] L. Del Buono,[16] B. Delaney,[65] H.-P. Dembinski,[19] J. Deng,[8] V. Denysenko,[51] O. Deschamps,[11] F. Dettori,[32,o] B. Dey,[78] P. Di Nezza,[28] I. Diachkov,[44] S. Didenko,[44] S. Ding,[69] Y. Ding,[50] L. Dittmann,[22] V. Dobishuk,[53] A. D. Docheva,[60] C. Dong,[4,m] A. M. Donohoe,[23] F. Dordei,[32] A. C. dos Reis,[2] A. D. Dowling,[69] W. Duan,[72] P. Duda,[82] M. W. Dudek,[41] L. Dufour,[49] V. Duk,[34] P. Durante,[49] M. M. Duras,[82] J. M. Durham,[68] O. D. Durmus,[78] A. Dziurda,[41] A. Dzyuba,[44] S. Easo,[58] E. Eckstein,[18] U. Egede,[1] A. Egorychev,[44] V. Egorychev,[44] S. Eisenhardt,[59] E. Ejopu,[63] L. Eklund,[84] M. Elashri,[66] J. Ellbracht,[19] S. Ely,[62] A. Ene,[43] J. Eschle,[69] S. Esen,[22] T. Evans,[38] F. Fabiano,[32] S. Faghih,[66] L. N. Falcao,[2] B. Fang,[7] R. Fantechi,[35] L. Fantini,[34,49,r] M. Faria,[50] K. Farmer,[59] D. Fazzini,[31,c] L. Felkowski,[82] M. Feng,[5,7] M. Feo,[19] A. Fernandez Casani,[48] M. Fernandez Gomez,[47] A. D. Fernez,[67] F. Ferrari,[25,j] F. Ferreira Rodrigues,[3] M. Ferrillo,[51] M. Ferro-Luzzi,[49] S. Filippov,[44] R. A. Fini,[24] M. Fiorini,[26,h] M. Firlej,[40] K. L. Fischer,[64] D. S. Fitzgerald,[86] C. Fitzpatrick,[63] T. Fiutowski,[40] F. Fleuret,[15] A. Fomin,[52] M. Fontana,[25] L. F. Foreman,[63] R. Forty,[49] D. Foulds-Holt,[59] V. Franco Lima,[3] M. Franco Sevilla,[67] M. Frank,[49] E. Franzoso,[26,h] G. Frau,[63] C. Frei,[49] D. A. Friday,[63] J. Fu,[7] Q. Führing,[19,56,b] Y. Fujii,[1] T. Fulghesu,[13] E. Gabriel,[38] G. Galati,[24] M. D. Galati,[38] A. Gallas Torreira,[47] D. Galli,[25,j] S. Gambetta,[59] M. Gandelman,[3] P. Gandini,[30] B. Ganie,[63] H. Gao,[7] R. Gao,[64] T. Q. Gao,[56] Y. Gao,[8] Y. Gao,[6] Y. Gao,[8] L. M. Garcia Martin,[50] P. Garcia Moreno,[45] J. García Pardiñas,[65] P. Gardner,[67] K. G. Garg,[8] L. Garrido,[45] C. Gaspar,[49] A. Gavrikov,[33] L. L. Gerken,[19] E. Gersabeck,[20] M. Gersabeck,[20] T. Gershon,[57] S. Ghizzo,[29,k] Z. Ghorbanimoghaddam,[55] L. Giambastiani,[33,g] F. I. Giasemis,[16,s] V. Gibson,[56] H. K. Giemza,[42] A. L. Gilman,[64] M. Giovannetti,[28] A. Gioventù,[45] L. Girardey,[63,58] M. A. Giza,[41] F. C. Glaser,[14,22] V. V. Gligorov,[16] C. Göbel,[70] L. Golinka-Bezshyyko,[85] E. Golobardes,[46] D. Golubkov,[44] A. Golutvin,[62,49] S. Gomez Fernandez,[45] W. Gomulka,[40] F. Goncalves Abrantes,[64] M. Goncerz,[41] G. Gong,[4,m] J. A. Gooding,[19] I. V. Gorelov,[44] C. Gotti,[31] E. Govorkova,[65] J. P. Grabowski,[18] L. A. Granado Cardoso,[49] E. Graugés,[45] E. Graverini,[50,t] L. Grazette,[57] G. Graziani,[27] A. T. Grecu,[43] L. M. Greeven,[38] N. A. Grieser,[66] L. Grillo,[60] S. Gromov,[44] C. Gu,[15] M. Guarise,[26] L. Guerry,[11] V. Guliaeva,[44] P. A. Günther,[22] A.-K. Guseinov,[50] E. Gushchin,[44] Y. Guz,[6,49] T. Gys,[49] K. Habermann,[18] T. Hadavizadeh,[1] C. Hadjivasiliou,[67] G. Haefeli,[50] C. Haen,[49] G. Hallett,[57] P. M. Hamilton,[67] J. Hammerich,[61] Q. Han,[33] X. Han,[22,49] S. Hansmann-Menzemer,[22] L. Hao,[7] N. Harnew,[64] T. H. Harris,[1] M. Hartmann,[14] S. Hashmi,[40] J. He,[7,u] F. Hemmer,[49] C. Henderson,[66] R. D. L. Henderson,[1] A. M. Hennequin,[49] K. Hennessy,[61] L. Henry,[50] J. Herd,[62] P. Herrero Gascon,[22] J. Heuel,[17] A. Hicheur,[3] G. Hijano Mendizabal,[51] J. Horswill,[63] R. Hou,[8] Y. Hou,[11] N. Howarth,[61] J. Hu,[72] W. Hu,[7] X. Hu,[4,m] W. Hulsbergen,[38] R. J. Hunter,[57] M. Hushchyn,[44] D. Hutchcroft,[61] M. Idzik,[40] D. Ilin,[44] P. Ilten,[66] A. Iniukhin,[44] A. Ishteev,[44] K. Ivshin,[44] H. Jage,[17] S. J. Jaimes Elles,[76,49,48] S. Jakobsen,[49] E. Jans,[38] B. K. Jashal,[48] A. Jawahery,[67] V. Jevtic,[19] E. Jiang,[67] X. Jiang,[5,7] Y. Jiang,[7] Y. J. Jiang,[6] M. John,[64] A. John Rubesh Rajan,[23] D. Johnson,[54] C. R. Jones,[56] T. P. Jones,[57] S. Joshi,[42] B. Jost,[49] J. Juan Castella,[56] N. Jurik,[49] I. Juszczak,[41] D. Kaminaris,[50] S. Kandybei,[52] M. Kane,[59] Y. Kang,[4,m] C. Kar,[11] M. Karacson,[49] D. Karpenkov,[44] A. Kauniskangas,[50] J. W. Kautz,[66] M. K. Kazanecki,[41] F. Keizer,[49] M. Kenzie,[56] T. Ketel,[38] B. Khanji,[69] A. Kharisova,[44] S. Kholodenko,[35,49] G. Khreich,[14] T. Kirn,[17] V. S. Kirsebom,[31,c] O. Kitouni,[65] S. Klaver,[39] N. Kleijne,[35,v] K. Klimaszewski,[42] M. R. Kmiec,[42] S. Koliiev,[53] L. Kolk,[19] A. Konoplyannikov,[6] P. Kopciewicz,[49] P. Koppenburg,[38] A. Korchin,[52] M. Korolev,[44] I. Kostiuk,[38] O. Kot,[53] S. Kotriakhova,

E. Kowalczyk,[67] A. Kozachuk,[44] P. Kravchenko,[44] L. Kravchuk,[44] M. Kreps,[57] P. Krokovny,[44] W. Krupa,[69] W. Krzemien,[42] O. Kshyvanskyi,[53] S. Kubis,[82] M. Kucharczyk,[41] V. Kudryavtsev,[44] E. Kulikova,[44] A. Kupsc,[84] V. Kushnir,[52] B. Kutsenko,[13] I. Kyryllin,[52] D. Lacarrere,[49] P. Laguarta Gonzalez,[45] A. Lai,[32] A. Lampis,[32] D. Lancierini,[62] C. Landesa Gomez,[47] J. J. Lane,[1] G. Lanfranchi,[28] C. Langenbruch,[22] J. Langer,[19] O. Lantwin,[44] T. Latham,[57] F. Lazzari,[35,49,t] C. Lazzeroni,[54] R. Le Gac,[13] H. Lee,[61] R. Lefèvre,[11] A. Leflat,[44] S. Legotin,[44] M. Lehuraux,[57] E. Lemos Cid,[49] O. Leroy,[13] T. Lesiak,[41] E. D. Lesser,[49] B. Leverington,[22] A. Li,[4,m] C. Li,[4] C. Li,[13] H. Li,[72] J. Li,[8] K. Li,[75] L. Li,[63] M. Li,[8] P. Li,[7] P.-R. Li,[73] Q. Li,[5,7] S. Li,[8] T. Li,[71] T. Li,[72] Y. Li,[8] Y. Li,[5] Z. Lian,[4,m] X. Liang,[69] S. Libralon,[48] C. Lin,[7] T. Lin,[58] R. Lindner,[49] H. Linton,[62] R. Litvinov,[32,49] D. Liu,[8] F. L. Liu,[1] G. Liu,[72] K. Liu,[73] S. Liu,[5,7] W. Liu,[8] Y. Liu,[59] Y. Liu,[73] Y. L. Liu,[62] G. Loachamin Ordonez,[70] A. Lobo Salvia,[45] A. Loi,[32] T. Long,[56] J. H. Lopes,[3] A. Lopez Huertas,[45] S. López Soliño,[47] Q. Lu,[15] C. Lucarelli,[27,w] D. Lucchesi,[33,g] M. Lucio Martinez,[48] Y. Luo,[6] A. Lupato,[33,x] E. Luppi,[26,h] K. Lynch,[23] X.-R. Lyu,[7] G. M. Ma,[4,m] S. Maccolini,[19] F. Machefert,[14] F. Maciuc,[43] B. Mack,[69] I. Mackay,[64] L. M. Mackey,[69] L. R. Madhan Mohan,[56] M. J. Madurai,[54] D. Magdalinski,[38] D. Maisuzenko,[44] J. J. Malczewski,[41] S. Malde,[64] L. Malentacca,[49] A. Malinin,[44] T. Maltsev,[44] G. Manca,[32,o] G. Mancinelli,[13] C. Mancuso,[14] R. Manera Escalero,[45] F. M. Manganella,[37] D. Manuzzi,[25] D. Marangotto,[30] J. F. Marchand,[10] R. Marchevski,[50] U. Marconi,[25] E. Mariani,[16] S. Mariani,[49] C. Marin Benito,[45] J. Marks,[22] A. M. Marshall,[55] L. Martel,[64] G. Martelli,[34] G. Martellotti,[36] L. Martinazzoli,[49] M. Martinelli,[31,c] D. Martinez Gomez,[80] D. Martinez Santos,[83] F. Martinez Vidal,[48] A. Martorell i Granollers,[46] A. Massafferri,[2] R. Matev,[49] A. Mathad,[49] V. Matiunin,[44] C. Matteuzzi,[69] K. R. Mattioli,[15] A. Mauri,[62] E. Maurice,[15] J. Mauricio,[45] P. Mayencourt,[50] J. Mazorra de Cos,[48] M. Mazurek,[42] M. McCann,[62] T. H. McGrath,[63] N. T. McHugh,[60] A. McNab,[63] R. McNulty,[23] B. Meadows,[66] G. Meier,[19] D. Melnychuk,[42] F. M. Meng,[4,m] M. Merk,[38,81] A. Merli,[50] L. Meyer Garcia,[67] D. Miao,[5,7] H. Miao,[7] M. Mikhasenko,[77] D. A. Milanes,[76,y] A. Minotti,[31,c] E. Minucci,[28] T. Miralles,[11] B. Mitreska,[19] D. S. Mitzel,[19] A. Modak,[58] L. Moeser,[19] R. A. Mohammed,[64] R. D. Moise,[17] E. F. Molina Cardenas,[86] T. Mombächer,[49] M. Monk,[57,1] S. Monteil,[11] A. Morcillo Gomez,[47] G. Morello,[28] M. J. Morello,[35,v] M. P. Morgenthaler,[22] J. Moron,[40] W. Morren,[38] A. B. Morris,[49] A. G. Morris,[13] R. Mountain,[69] H. Mu,[4,m] Z. M. Mu,[6] E. Muhammad,[57] F. Muheim,[59] M. Mulder,[80] K. Müller,[51] F. Muñoz-Rojas,[9] R. Murta,[62] V. Mytrochenko,[52] P. Naik,[61] T. Nakada,[50] R. Nandakumar,[58] T. Nanut,[49] I. Nasteva,[3] M. Needham,[59] E. Nekrasova,[44] N. Neri,[30,l] S. Neubert,[18] N. Neufeld,[49] P. Neustroev,[44] J. Nicolini,[49] D. Nicotra,[81] E. M. Niel,[15] N. Nikitin,[44] Q. Niu,[73] P. Nogarolli,[3] P. Nogga,[18] C. Normand,[55] J. Novoa Fernandez,[47] G. Nowak,[66] C. Nunez,[86] H. N. Nur,[60] A. Oblakowska-Mucha,[40] V. Obraztsov,[44] T. Oeser,[17] S. Okamura,[26,h] A. Okhotnikov,[44] O. Okhrimenko,[53] R. Oldeman,[32,o] F. Oliva,[59] M. Olocco,[19] C. J. G. Onderwater,[81] R. H. O'Neil,[49] D. Osthues,[19] J. M. Otalora Goicochea,[3] P. Owen,[51] A. Oyanguren,[48] O. Ozcelik,[59] F. Paciolla,[35,z] A. Padee,[42] K. O. Padeken,[18] B. Pagare,[47] T. Pajero,[49] A. Palano,[24] M. Palutan,[28] X. Pan,[4,m] S. Panebianco,[12] G. Panshin,[5] L. Paolucci,[57] A. Papanestis,[58,49] M. Pappagallo,[24,q] L. L. Pappalardo,[26] C. Pappenheimer,[66] C. Parkes,[63] D. Parmar,[77] B. Passalacqua,[26,h] G. Passaleva,[27] D. Passaro,[35,49,v] A. Pastore,[24] M. Patel,[62] J. Patoc,[64] C. Patrignani,[25,j] A. Paul,[69] C. J. Pawley,[81] A. Pellegrino,[38] J. Peng,[5,7] M. Pepe Altarelli,[28] S. Perazzini,[25] D. Pereima,[44] H. Pereira Da Costa,[68] A. Pereiro Castro,[47] P. Perret,[11] A. Perrevoort,[80] A. Perro,[49,13] M. J. Peters,[66] K. Petridis,[55] A. Petrolini,[29,k] J. P. Pfaller,[66] H. Pham,[69] L. Pica,[35] M. Piccini,[34] L. Piccolo,[32] B. Pietrzyk,[10] G. Pietrzyk,[14] R. N. Pilato,[61] D. Pinci,[36] F. Pisani,[49] M. Pizzichemi,[31,49,c] V. M. Placinta,[43] M. Plo Casasus,[47] T. Poeschl,[49] F. Polci,[16] M. Poli Lener,[28] A. Poluektov,[13] N. Polukhina,[44] I. Polyakov,[63] E. Polycarpo,[3] S. Ponce,[49] D. Popov,[7,49] S. Poslavskii,[44] K. Prasanth,[59] C. Prouve,[83] D. Provenzano,[32,o] V. Pugatch,[53] G. Punzi,[35,t] S. Qasim,[51] Q. Q. Qian,[6] W. Qian,[7] N. Qin,[4,m] S. Qu,[4,m] R. Quagliani,[49] R. I. Rabadan Trejo,[57] J. H. Rademacker,[55] M. Rama,[35] M. Ramírez García,[86] V. Ramos De Oliveira,[70] M. Ramos Pernas,[57] M. S. Rangel,[3] F. Ratnikov,[44] G. Raven,[39] M. Rebollo De Miguel,[48] F. Redi,[30,x] J. Reich,[55] F. Reiss,[20] Z. Ren,[7] P. K. Resmi,[64] M. Ribalda Galvez,[45] R. Ribatti,[50] G. Ricart,[15,12] D. Riccardi,[35,v] S. Ricciardi,[58] K. Richardson,[65] M. Richardson-Slipper,[59] K. Rinnert,[61] P. Robbe,[14,49] G. Robertson,[60] E. Rodrigues,[61] A. Rodriguez Alvarez,[45] E. Rodriguez Fernandez,[47] J. A. Rodriguez Lopez,[76] E. Rodriguez Rodriguez,[49] J. Roensch,[19] A. Rogachev,[44] A. Rogovskiy,[58] D. L. Rolf,[19] P. Roloff,[49] V. Romanovskiy,[66] A. Romero Vidal,[47] G. Romolini,[26]

F. Ronchetti,[50] T. Rong,[6] M. Rotondo,[28] S. R. Roy,[22] M. S. Rudolph,[69] M. Ruiz Diaz,[22] R. A. Ruiz Fernandez,[47] J. Ruiz Vidal,[81] J. J. Saavedra-Arias,[9] J. J. Saborido Silva,[47] R. Sadek,[15] N. Sagidova,[44] D. Sahoo,[78] N. Sahoo,[54] B. Saitta,[32,o] M. Salomoni,[31,49,c] I. Sanderswood,[48] R. Santacesaria,[36] C. Santamarina Rios,[47] M. Santimaria,[28] L. Santoro,[2] E. Santovetti,[37] A. Saputi,[26,49] D. Saranin,[44] A. Sarnatskiy,[80] G. Sarpis,[59] M. Sarpis,[79] C. Satriano,[36,aa] A. Satta,[37] M. Saur,[73] D. Savrina,[44] H. Sazak,[17] F. Sborzacchi,[49,28] A. Scarabotto,[19] S. Schael,[17] S. Scherl,[61] M. Schiller,[22] H. Schindler,[49] M. Schmelling,[21] B. Schmidt,[49] S. Schmitt,[17] H. Schmitz,[18] O. Schneider,[50] A. Schopper,[62] N. Schulte,[19] S. Schulte,[50] M. H. Schune,[14] G. Schwering,[17] B. Sciascia,[28] A. Sciuccati,[49] I. Segal,[77] S. Sellam,[47] A. Semennikov,[44] T. Senger,[51] M. Senghi Soares,[39] A. Sergi,[29,k] N. Serra,[51] L. Sestini,[27] A. Seuthe,[19] B. Sevilla Sanjuan,[46] Y. Shang,[6] D. M. Shangase,[86] M. Shapkin,[44] R. S. Sharma,[69] I. Shchemerov,[44] L. Shchutska,[50] T. Shears,[61] L. Shekhtman,[44] Z. Shen,[38] S. Sheng,[5,7] V. Shevchenko,[44] B. Shi,[7] Q. Shi,[7] Y. Shimizu,[14] E. Shmanin,[25] R. Shorkin,[44] J. D. Shupperd,[69] R. Silva Coutinho,[69] G. Simi,[33,g] S. Simone,[24,q] M. Singha,[78] N. Skidmore,[57] T. Skwarnicki,[69] M. W. Slater,[54] E. Smith,[65] K. Smith,[68] M. Smith,[62] L. Soares Lavra,[59] M. D. Sokoloff,[66] F. J. P. Soler,[60] A. Solomin,[55] A. Solovev,[44] N. S. Sommerfeld,[18] R. Song,[1] Y. Song,[50] Y. Song,[4,m] Y. S. Song,[6] F. L. Souza De Almeida,[69] B. Souza De Paula,[3] E. Spadaro Norella,[29,k] E. Spedicato,[25] J. G. Speer,[19] E. Spiridenkov,[44] P. Spradlin,[60] V. Sriskaran,[49] F. Stagni,[49] M. Stahl,[77] S. Stahl,[49] S. Stanislaus,[64] M. Stefaniak,[87] E. N. Stein,[49] O. Steinkamp,[51] O. Stenyakin,[44] H. Stevens,[19] D. Strekalina,[44] Y. Su,[7] F. Suljik,[64] J. Sun,[32] L. Sun,[74] D. Sundfeld,[2] W. Sutcliffe,[51] K. Swientek,[40] F. Swystun,[56] A. Szabelski,[42] T. Szumlak,[40] Y. Tan,[4,m] Y. Tang,[74] Y. T. Tang,[7] M. D. Tat,[22] A. Terentev,[44] F. Terzuoli,[35,49,z] F. Teubert,[49] U. Thoma,[18] E. Thomas,[49] D. J. D. Thompson,[54] H. Tilquin,[62] V. Tisserand,[11] S. T'Jampens,[10] M. Tobin,[5] L. Tomassetti,[26,h] G. Tonani,[30] X. Tong,[6] T. Tork,[30] D. Torres Machado,[2] L. Toscano,[19] D. Y. Tou,[4,m] C. Trippl,[46] G. Tuci,[22] N. Tuning,[38] L. H. Uecker,[22] A. Ukleja,[40] D. J. Unverzagt,[22] A. Upadhyay,[49] B. Urbach,[59] A. Usachov,[39] A. Ustyuzhanin,[44] U. Uwer,[22] V. Vagnoni,[25] V. Valcarce Cadenas,[47] G. Valenti,[25] N. Valls Canudas,[49] J. van Eldik,[49] H. Van Hecke,[68] E. van Herwijnen,[62] C. B. Van Hulse,[47,bb] R. Van Laak,[50] M. van Veghel,[38] G. Vasquez,[51] R. Vazquez Gomez,[45] P. Vazquez Regueiro,[47] C. Vázquez Sierra,[83] S. Vecchi,[26] J. J. Velthuis,[55] M. Veltri,[27,cc] A. Venkateswaran,[50] M. Verdoglia,[32] M. Vesterinen,[57] D. Vico Benet,[64] P. Vidrier Villalba,[45] M. Vieites Diaz,[47] X. Vilasis-Cardona,[46] E. Vilella Figueras,[61] A. Villa,[25] P. Vincent,[16] B. Vivacqua,[3] F. C. Volle,[54] D. vom Bruch,[13] N. Voropaev,[44] K. Vos,[81] C. Vrahas,[59] J. Wagner,[19] J. Walsh,[35] E. J. Walton,[1,57] G. Wan,[6] A. Wang,[7] C. Wang,[22] G. Wang,[8] H. Wang,[73] J. Wang,[6] J. Wang,[5] J. Wang,[4,m] J. Wang,[74] M. Wang,[49] N. W. Wang,[7] R. Wang,[55] X. Wang,[8] X. Wang,[72] X. W. Wang,[62] Y. Wang,[75] Y. Wang,[6] Y. W. Wang,[73] Z. Wang,[14] Z. Wang,[4,m] Z. Wang,[30] J. A. Ward,[57,1] M. Waterlaat,[49] N. K. Watson,[54] D. Websdale,[62] Y. Wei,[6] J. Wendel,[83] B. D. C. Westhenry,[55] C. White,[56] M. Whitehead,[60] E. Whiter,[54] A. R. Wiederhold,[63] D. Wiedner,[19] G. Wilkinson,[64,49] M. K. Wilkinson,[66] M. Williams,[65] M. J. Williams,[49] M. R. J. Williams,[59] R. Williams,[56] Z. Williams,[55] F. F. Wilson,[58] M. Winn,[12] W. Wislicki,[42] M. Witek,[41] L. Witola,[19] G. Wormser,[14] S. A. Wotton,[56] H. Wu,[69] J. Wu,[8] X. Wu,[74] Y. Wu,[6,56] Z. Wu,[7] K. Wyllie,[49] S. Xian,[72] Z. Xiang,[5] Y. Xie,[8] T. X. Xing,[30] A. Xu,[35,v] L. Xu,[4,m] L. Xu,[4,m] M. Xu,[49] Z. Xu,[49] Z. Xu,[7] Z. Xu,[5] K. Yang,[62] X. Yang,[6] Y. Yang,[29] Z. Yang,[6] V. Yeroshenko,[14] H. Yeung,[63] H. Yin,[8] X. Yin,[7] C. Y. Yu,[6] J. Yu,[71] X. Yuan,[5] Y Yuan,[5,7] E. Zaffaroni,[50] M. Zavertyaev,[21] M. Zdybal,[41] F. Zenesini,[25] C. Zeng,[5,7] M. Zeng,[4,m] C. Zhang,[6] D. Zhang,[8] J. Zhang,[7] L. Zhang,[4,m] R. Zhang,[8] S. Zhang,[71] S. Zhang,[64] Y. Zhang,[6] Y. Z. Zhang,[4,m] Z. Zhang,[4,m] Y. Zhao,[22] A. Zhelezov,[22] S. Z. Zheng,[6] X. Z. Zheng,[4,m] Y. Zheng,[7] T. Zhou,[6] X. Zhou,[8] Y. Zhou,[7] V. Zhovkovska,[57] L. Z. Zhu,[7] X. Zhu,[4,m] X. Zhu,[8] Y. Zhu,[17] V. Zhukov,[17] J. Zhuo,[48] Q. Zou,[5,7] D. Zuliani,[33,g] and G. Zunica[50]

(LHCb Collaboration)

[1]*School of Physics and Astronomy, Monash University, Melbourne, Australia*
[2]*Centro Brasileiro de Pesquisas Físicas (CBPF), Rio de Janeiro, Brazil*
[3]*Universidade Federal do Rio de Janeiro (UFRJ), Rio de Janeiro, Brazil*
[4]*Department of Engineering Physics, Tsinghua University, Beijing, China*

[5]Institute Of High Energy Physics (IHEP), Beijing, China
[6]School of Physics State Key Laboratory of Nuclear Physics and Technology, Peking University, Beijing, China
[7]University of Chinese Academy of Sciences, Beijing, China
[8]Institute of Particle Physics, Central China Normal University, Wuhan, Hubei, China
[9]Consejo Nacional de Rectores (CONARE), San Jose, Costa Rica
[10]Université Savoie Mont Blanc, CNRS, IN2P3-LAPP, Annecy, France
[11]Université Clermont Auvergne, CNRS/IN2P3, LPC, Clermont-Ferrand, France
[12]Université Paris-Saclay, Centre d'Etudes de Saclay (CEA), IRFU, Saclay, France, Gif-Sur-Yvette, France
[13]Aix Marseille Univ, CNRS/IN2P3, CPPM, Marseille, France
[14]Université Paris-Saclay, CNRS/IN2P3, IJCLab, Orsay, France
[15]Laboratoire Leprince-Ringuet, CNRS/IN2P3, Ecole Polytechnique, Institut Polytechnique de Paris, Palaiseau, France
[16]LPNHE, Sorbonne Université, Paris Diderot Sorbonne Paris Cité, CNRS/IN2P3, Paris, France
[17]I. Physikalisches Institut, RWTH Aachen University, Aachen, Germany
[18]Universität Bonn - Helmholtz-Institut für Strahlen und Kernphysik, Bonn, Germany
[19]Fakultät Physik, Technische Universität Dortmund, Dortmund, Germany
[20]Physikalisches Institut, Albert-Ludwigs-Universität Freiburg, Freiburg, Germany
[21]Max-Planck-Institut für Kernphysik (MPIK), Heidelberg, Germany
[22]Physikalisches Institut, Ruprecht-Karls-Universität Heidelberg, Heidelberg, Germany
[23]School of Physics, University College Dublin, Dublin, Ireland
[24]INFN Sezione di Bari, Bari, Italy
[25]INFN Sezione di Bologna, Bologna, Italy
[26]INFN Sezione di Ferrara, Ferrara, Italy
[27]INFN Sezione di Firenze, Firenze, Italy
[28]INFN Laboratori Nazionali di Frascati, Frascati, Italy
[29]INFN Sezione di Genova, Genova, Italy
[30]INFN Sezione di Milano, Milano, Italy
[31]INFN Sezione di Milano-Bicocca, Milano, Italy
[32]INFN Sezione di Cagliari, Monserrato, Italy
[33]INFN Sezione di Padova, Padova, Italy
[34]INFN Sezione di Perugia, Perugia, Italy
[35]INFN Sezione di Pisa, Pisa, Italy
[36]INFN Sezione di Roma La Sapienza, Roma, Italy
[37]INFN Sezione di Roma Tor Vergata, Roma, Italy
[38]Nikhef National Institute for Subatomic Physics, Amsterdam, Netherlands
[39]Nikhef National Institute for Subatomic Physics and VU University Amsterdam, Amsterdam, Netherlands
[40]AGH - University of Krakow, Faculty of Physics and Applied Computer Science, Kraków, Poland
[41]Henryk Niewodniczanski Institute of Nuclear Physics Polish Academy of Sciences, Kraków, Poland
[42]National Center for Nuclear Research (NCBJ), Warsaw, Poland
[43]Horia Hulubei National Institute of Physics and Nuclear Engineering, Bucharest-Magurele, Romania
[44]Authors affiliated with an institute formerly covered by a cooperation agreement with CERN
[45]ICCUB, Universitat de Barcelona, Barcelona, Spain
[46]La Salle, Universitat Ramon Llull, Barcelona, Spain
[47]Instituto Galego de Física de Altas Enerxías (IGFAE), Universidade de Santiago de Compostela, Santiago de Compostela, Spain
[48]Instituto de Fisica Corpuscular, Centro Mixto Universidad de Valencia - CSIC, Valencia, Spain
[49]European Organization for Nuclear Research (CERN), Geneva, Switzerland
[50]Institute of Physics, Ecole Polytechnique Fédérale de Lausanne (EPFL), Lausanne, Switzerland
[51]Physik-Institut, Universität Zürich, Zürich, Switzerland
[52]NSC Kharkiv Institute of Physics and Technology (NSC KIPT), Kharkiv, Ukraine
[53]Institute for Nuclear Research of the National Academy of Sciences (KINR), Kyiv, Ukraine
[54]School of Physics and Astronomy, University of Birmingham, Birmingham, United Kingdom
[55]H.H. Wills Physics Laboratory, University of Bristol, Bristol, United Kingdom
[56]Cavendish Laboratory, University of Cambridge, Cambridge, United Kingdom
[57]Department of Physics, University of Warwick, Coventry, United Kingdom
[58]STFC Rutherford Appleton Laboratory, Didcot, United Kingdom
[59]School of Physics and Astronomy, University of Edinburgh, Edinburgh, United Kingdom
[60]School of Physics and Astronomy, University of Glasgow, Glasgow, United Kingdom
[61]Oliver Lodge Laboratory, University of Liverpool, Liverpool, United Kingdom
[62]Imperial College London, London, United Kingdom
[63]Department of Physics and Astronomy, University of Manchester, Manchester, United Kingdom
[64]Department of Physics, University of Oxford, Oxford, United Kingdom

[65]Massachusetts Institute of Technology, Cambridge, Massachusetts, USA
[66]University of Cincinnati, Cincinnati, Ohio, USA
[67]University of Maryland, College Park, Maryland, USA
[68]Los Alamos National Laboratory (LANL), Los Alamos, New Mexico, USA
[69]Syracuse University, Syracuse, New York, USA
[70]Pontifícia Universidade Católica do Rio de Janeiro (PUC-Rio), Rio de Janeiro, Brazil
(associated with Universidade Federal do Rio de Janeiro (UFRJ), Rio de Janeiro, Brazil)
[71]School of Physics and Electronics, Hunan University, Changsha City, China
(associated with Institute of Particle Physics, Central China Normal University, Wuhan, Hubei, China)
[72]Guangdong Provincial Key Laboratory of Nuclear Science, Guangdong-Hong Kong Joint Laboratory of Quantum Matter, Institute of Quantum Matter, South China Normal University, Guangzhou, China
(associated with Department of Engineering Physics, Tsinghua University, Beijing, China)
[73]Lanzhou University, Lanzhou, China
(associated with Institute of High Energy Physics (IHEP), Beijing, China)
[74]School of Physics and Technology, Wuhan University, Wuhan, China
(associated with Department of Engineering Physics, Tsinghua University, Beijing, China)
[75]Henan Normal University, Xinxiang, China
(associated with Institution No. 8)
[76]Departamento de Fisica, Universidad Nacional de Colombia, Bogota, Colombia
(associated with LPNHE, Sorbonne Université, Paris Diderot Sorbonne Paris Cité, CNRS/IN2P3, Paris, France)
[77]Ruhr Universitaet Bochum, Fakultaet f. Physik und Astronomie, Bochum, Germany
(associated with Fakultät Physik, Technische Universität Dortmund, Dortmund, Germany)
[78]Eotvos Lorand University, Budapest, Hungary
(associated with European Organization for Nuclear Research (CERN), Geneva, Switzerland)
[79]Faculty of Physics, Vilnius University, Vilnius, Lithuania
(associated with Physikalisches Institut, Albert-Ludwigs-Universität Freiburg, Freiburg, Germany)
[80]Van Swinderen Institute, University of Groningen, Groningen, Netherlands
(associated with Nikhef National Institute for Subatomic Physics, Amsterdam, Netherlands)
[81]Universiteit Maastricht, Maastricht, Netherlands
(associated with Nikhef National Institute for Subatomic Physics, Amsterdam, Netherlands)
[82]Tadeusz Kosciuszko Cracow University of Technology, Cracow, Poland
(associated with Henryk Niewodniczanski Institute of Nuclear Physics Polish Academy of Sciences, Kraków, Poland)
[83]Universidade da Coruña, A Coruña, Spain
(associated with La Salle, Universitat Ramon Llull, Barcelona, Spain)
[84]Department of Physics and Astronomy, Uppsala University, Uppsala, Sweden
(associated with School of Physics and Astronomy, University of Glasgow, Glasgow, United Kingdom)
[85]Taras Schevchenko University of Kyiv, Faculty of Physics, Kyiv, Ukraine
(associated with Université Paris-Saclay, CNRS/IN2P3, IJCLab, Orsay, France)
[86]University of Michigan, Ann Arbor, Michigan, USA
(associated with Syracuse University, Syracuse, New York, USA)
[87]Ohio State University, Columbus, Ohio, USA
(associated with Los Alamos National Laboratory (LANL), Los Alamos, New Mexico, USA)

[a]Deceased.
[b]Also at Lamarr Institute for Machine Learning and Artificial Intelligence, Dortmund, Germany.
[c]Also at Università degli Studi di Milano-Bicocca, Milano, Italy.
[d]Also at Università di Roma Tor Vergata, Roma, Italy.
[e]Also at Università di Modena e Reggio Emilia, Modena, Italy.
[f]Also at Department of Physics and Astronomy, University of Victoria, Victoria, Canada.
[g]Also at Università di Padova, Padova, Italy.
[h]Also at Università di Ferrara, Ferrara, Italy.
[i]Also at Facultad de Ciencias Fisicas, Madrid, Spain.
[j]Also at Università di Bologna, Bologna, Italy.
[k]Also at Università di Genova, Genova, Italy.
[l]Also at Università degli Studi di Milano, Milano, Italy.
[m]Also at Center for High Energy Physics, Tsinghua University, Beijing, China.
[n]Also at Universidad Nacional Autónoma de Honduras, Tegucigalpa, Honduras.
[o]Also at Università di Cagliari, Cagliari, Italy.
[p]Also at Centro Federal de Educacão Tecnológica Celso Suckow da Fonseca, Rio De Janeiro, Brazil.
[q]Also at Università di Bari, Bari, Italy.

[r]Also at Università di Perugia, Perugia, Italy.
[s]Also at LIP6, Sorbonne Université, Paris, France.
[t]Also at Università di Pisa, Pisa, Italy.
[u]Also at Hangzhou Institute for Advanced Study, UCAS, Hangzhou, China.
[v]Also at Scuola Normale Superiore, Pisa, Italy.
[w]Also at Università di Firenze, Firenze, Italy.
[x]Also at Università di Bergamo, Bergamo, Italy.
[y]Also at Universidad de Ingeniería y Tecnología (UTEC), Lima, Peru.
[z]Also at Università di Siena, Siena, Italy.
[aa]Also at Università della Basilicata, Potenza, Italy.
[bb]Also at Universidad de Alcalá, Alcalá de Henares, Spain.
[cc]Also at Università di Urbino, Urbino, Italy.